33rd EPS Conference on Plasma Phys. Rome, 19 - 23 June 2006 ECA Vol.**30I**, P-5.156 (2006)

Contour dynamics modelling of collisionless magnetic reconnection

E.V. van der Plas, L.P.J. Kamp[1] and H.J. de Blank

FOM Institute for Plasma Physics Rijnhuizen, Association Euratom-FOM, Trilateral Euregio Cluster, P.O. Box 1207, 3430 BE Nieuwegein, The Netherlands, `www.rijnh.nl`

[1] *Department of Applied Physics, Technical University of Eindhoven, P.O. Box 513, 5600 MB Eindhoven, The Netherlands*

Introduction Fast magnetic reconnection is responsible for some of the more violent plasma phenomena, such as magnetic substorms in the earth's magnetosphere and the internal disruptions, the so-called sawteeth in fusion experiments. Effects of finite electron inertia and parallel compressibility can enhance the reconnection over the rate given by resistivity. This becomes relevant in very hot as well as very dilute plasmas. The in this way calculated reconnection rates are comparable with those estimated from fusion experiments[1].

Two-fluid modelling of the tearing instability of a straight current layer has shown that current and vorticity gradients increase faster than exponentially and length scales shrink well below the intrinsic scales of the system (skin depth, ion gyroradius)[2,3].

An analytical treatment of a tearing mode in a straight current slab has been made possible by considering an equilibrium that consists of piecewise uniform regions of current density. This analysis can be extended to cylindrical geometry so that the linear stability of an annular region of generalized current density can be studied.

In this paper we apply the method of contour dynamics [4,5] to follow the dynamics of a reconnecting tearing mode into the nonlinear regime.

Drift-Alfvén model We consider a strongly magnetized, low β plasma, with a strong magnetic guide field $\mathbf{B} = B_0(\mathbf{e}_z + \mathbf{e}_z \times \nabla\psi)$ and an electric field $\mathbf{E} = B_0(\mathbf{e}_z \partial_t \psi - \nabla\phi)$, where ϕ, ψ are the electrostatic and magnetic vector potential, respectively. The plasma is described as an electron and an ion fluid. The electrons are assumed to be collisionless, and their inertia in the direction parallel to the magnetic field is taken into account. The ion response is modelled by a cold ion approximation, that does not involve ion dynamics but couples parallel perturbations in the electron fluid to quasi-neutrality. Parallel current is carried by electrons only. The continuity and momentum balance equations,

$$\partial_t \nabla^2\phi + [\phi, \nabla^2\phi] = v_A^2[\psi, \tilde{\nabla}^2\psi], \tag{1}$$

$$\partial_t(\tilde{\nabla}^2\psi) + [\phi, \tilde{\nabla}^2\psi] = -\frac{\rho_s^2}{d_e^2}[\nabla^2\phi, \psi], \tag{2}$$

with $[A,B] = \mathbf{e}_z \cdot \nabla A \times \nabla B$, $\tilde{\nabla}^2 = \nabla^2 - d_e^{-2}$, $v_A^2 = B_0^2/m_i n_0$ the Alfvén velocity and $d_e = c/\omega_{pe}$ the electron inertial skin depth.

These equations can be cast in the form of two purely advective equations for generalized vorticities [6], that are being advected by their own respective generalized streamfunction,

$$\partial_t \omega_\pm + [\phi_\pm, \omega_\pm] = 0. \tag{3}$$

The vorticities are given by $\omega_\pm = \nabla^2\phi \pm (v_A/v_{th})^2\tilde{\nabla}^2 v_{th}\psi$, and their streamfunctions by $\phi_\pm = \phi \pm v_{th}\psi$.

Contour Dynamics This formulation allows the simplification that is exploited when using contour dynamics. Inverting the definition for the generalized vorticity, we obtain the stream function as integrals over the vorticity distributions $\omega_{\pm}(\mathbf{r})$,

$$\phi_\alpha(\mathbf{r}) = \sum_\beta \int d^2r' \Phi_{\alpha\beta}(|\mathbf{r}-\mathbf{r}'|)\omega_\beta(\mathbf{r}'), \tag{4}$$

where $\alpha, \beta = +, -$ denotes the type of vorticity, and with the Green's function for the unbounded domain, given by

$$\Phi_{\alpha,\beta}(r) = \frac{1}{2\pi}\Big(\ln r + c_\alpha c_\beta K_0(\frac{r}{d_e})\Big),$$

with $c_\pm = \pm v_{th}/v_A$ and K_0 is the modified Bessel function of the second kind. By assuming the (generalized) vorticity to be constant within a well-defined region C, bounded by a contour ∂C, the dynamics is completely defined. The velocity of the n-th contour is calculated by evaluating

$$v_n(\mathbf{r}) = -\sum_m \omega_m \oint_{\partial C_m} d\mathbf{l}' \Phi_{\beta(n)\beta(m)}(|\mathbf{r}-\mathbf{r}'|),$$

where the summation is over all contours ∂C_m and $\beta(m)$ is the type of the m-th contour. Because the surface enclosed by ∂C_m is conserved, all linear combinations of fluxes ω_α are conserved. This makes this approach very suitable for numerical purposes, as there are no external boundary conditions to be observed.

By superposing contours of the $+$ and $-$ type we can construct regions of pure current density by giving them opposite weight.

Geometry, linear stability We construct an equilibrium with a ,z-independent cylindrical geometry, by making a linear combination of two concentric patches of radius R_j, i.e. four ω_α contours, with vanishing vorticity and with magnetic vector potential

$$\psi_{0,j} = -d_e^2 j_j \begin{cases} 1 - \frac{R_j}{d_e}K_1(\frac{R_j}{d_e})I_0(\frac{r}{d_e}) & \text{if } r < R_j, \\ \frac{R_j}{d_e}I_1(\frac{R_j}{d_e})K_0(\frac{r}{d_e}) & \text{if } r > R_j, \end{cases}$$

with I_i, K_i modified Bessel functions of the first and second kind. We obtain a positive current in the annular region between $R_1 < r < R_2$ for $\psi_0 = \psi_{0,1} + \psi_{0,2}$, with $j_1 < 0 < j_2$.

We introduce linear perturbations of the contours of these patches of the form $\mathbf{A}(r,\theta) = A_0(r)\exp(i(m\theta - \omega t)$. When we linearize eqs. (1, 2) we obtain the system

$$-\omega\nabla^2\phi_1 = v_A^2 \frac{m}{r}\left\{(\psi_0')(\tilde{\nabla}^2\psi_1) - (\tilde{\nabla}^2\psi_0)'(\psi_1)\right\}, \tag{5}$$

$$-\omega d_e^2\tilde{\nabla}^2\psi_1 = d_e^2\frac{m}{r}\phi_1(\tilde{\nabla}^2\psi_0)' + \rho_s^2\frac{m}{r}(\nabla^2\phi_1)\psi_0', \tag{6}$$

where prime denotes derivation with respect to r. The contours of a current patch are perturbed at R_i by

$$\phi_{i,m}(r) = \frac{\phi_{i,m}}{2m}\begin{cases}\left(\frac{r}{R_i}\right)^m \\ \left(\frac{R_i}{r}\right)^m\end{cases} \quad \text{and} \quad \psi_{i,m}(r) = \psi_{i,m}\begin{cases} K_m(\frac{R_i}{d_e})I_m(\frac{r}{d_e}) & \text{if } r < R_i, \\ I_m(\frac{R_i}{d_e})K_m(\frac{r}{d_e}) & \text{if } r > R_i, \end{cases}$$

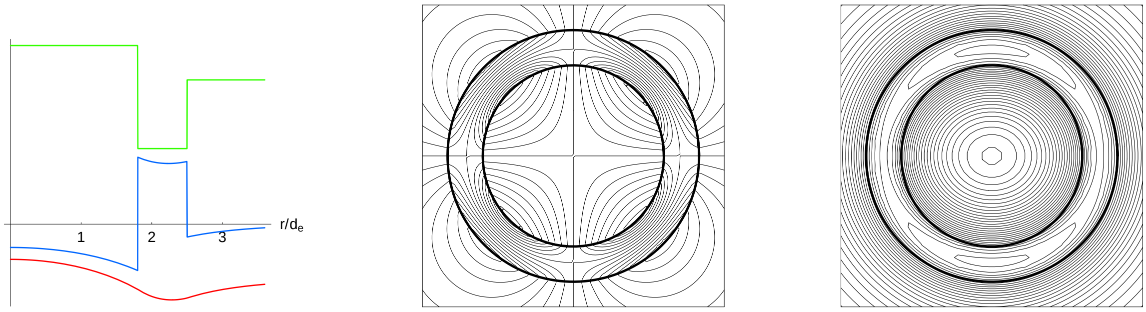

Figure 1: Left: the equilibrium geometry. The upper curve shows the r-dependence of v_z. The central curve is the current density $\nabla^2\psi_0(r)$, showing a current layer at $R_1 < r < R_2$ and screening at distances $> d_e$. The lower curve is ψ_0. Middle and right are the ϕ and ψ-fields of a linear perturbation.

with $\tilde{k} = \sqrt{k^2 + d_e^{-2}}$. This yields a dispersion relation in ω and k,

$$\omega^4 + \omega^2 \mathrm{Tr}(M) + \det(M) = 0,$$

with

$$M = -\frac{m}{2} v_A^2 \begin{pmatrix} j_1 I_{m1} K_{m1} - \hat{j}_1 & j_1 I_{m1} K_{m2} \\ j_2 I_{m1} K_{m2} & j_1 I_{m2} K_{m2} - \hat{j}_2 \end{pmatrix} \begin{pmatrix} j_1 - 2m\hat{j}_1 \rho_s^2/d_e^2 & j_1 (R_1/R_2)^m \\ j_2 (R_1/R_2)^m & j_2 - 2m\hat{j}_2 \rho_s^2/d_e^2 \end{pmatrix}$$

and

$$\hat{j}_1 = \frac{\psi_0'(R_1)}{R_1} = j_1 I_{11} K_{11} + j_2 I_{11} K_{12} \frac{R_2}{R_1},$$
$$\hat{j}_2 = \frac{\psi_0'(R_2)}{R_2} = j_1 I_{11} K_{12} \frac{R_1}{R_2} + j_2 I_{12} K_{12},$$

and $K_{mi} = K_m(R_i/d_e), I_{mi} = I_m(R_i/d_e)$, $i = 1, 2$.

We can identify three qualitatively different regimes in this description, with different stability characteristics. For $\mathrm{Tr}(M), \det(M) > 0$ we have two unstable modes, for $\det(M) < 0$ we have one unstable mode and for $0 < \det(M) < \frac{1}{4}\mathrm{Tr}(M)^2$ the current channel is stable.

Numerical method, results We consider an equilibrium with $R_1 = 1.8 d_e$, $R_2 = 2.5 d_e$ and $\rho_s = d_e$ (see left figure in Fig. 1). The ratio of the jumps in the current density jumps at R_1 and R_2 of the original patches, $j_1/j_2 = -1.$, determines that the resonance layer $\nabla\psi = 0$ is located between R_1 and R_2. For these parameters the $m = 2$ mode with tearing parity is unstable. The $m = 2$ kink mode is stable.

The contour dynamics code [4,5] involves the symplectic time integration of quasi-uniformly distributed nodes along the predescribed contours. The equilibrium contours are initially pertubed with an $m = 2$ seed displacement of the outer contours of amplitude $0.004 R_2$

When we do this, the at first overlapping contours are drawn apart, creating regions of positive and negative vorticity. In this way a $m = 2$ tearing type mode develops that qualitatively looks like the analytic linear mode. We observe that the mode does not nonlinearly saturate: it keeps growing until all of the magnetic field in the central region is reconnected (compare fig. 1 and fig. 2, $t = 100\tau_A$). This is due to the vanishing central magnetic shear of this model equilibrium. In this way, the o-point regions become current filaments, that eventually, for $t > 200\tau_A$, start to merge, as described in [7]. Later, for $t > 250\tau_A$, very thin filamentary structures emerge as

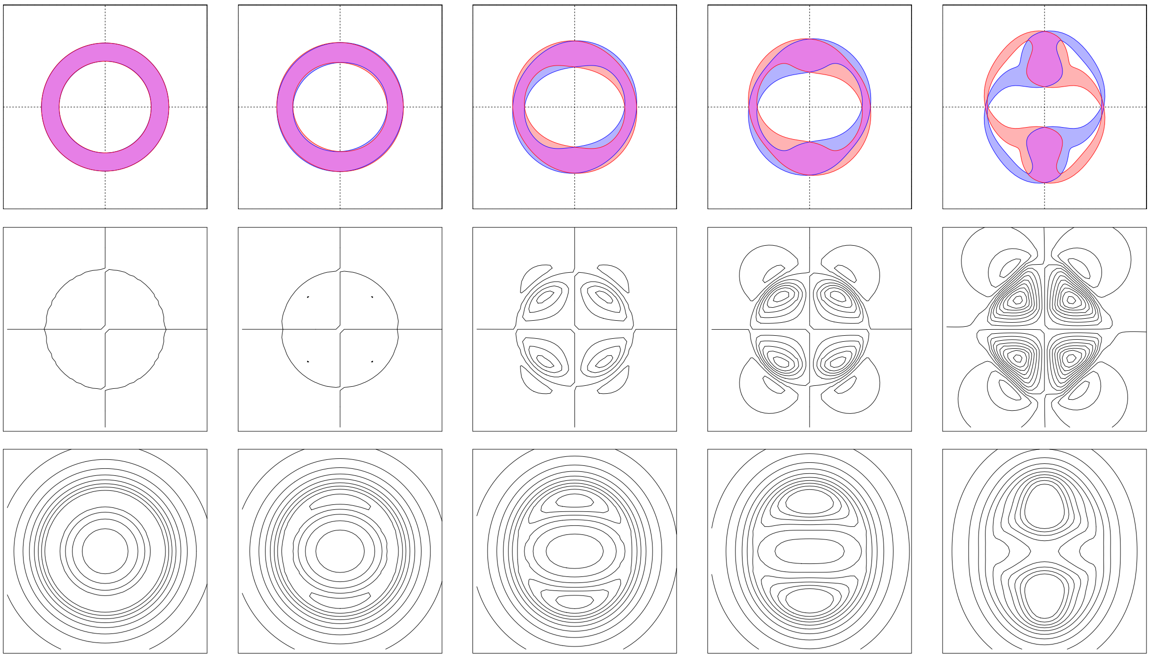

Figure 2: Contour dynamics simulation. From left to right the contours of $\omega_\pm$ (red, blue), after $t/\tau_A = 45$, 100, 140, 160, and 200. Second row the ϕ and the third row the ψ-contours.

the current patches are stretched and folded. The numerical challenges this poses have been adressed in [5] by means of contour surgery.

Until $t = 200\tau_A$ current layer in the x-point region continually narrows, but subsequently the in-out asymmetry of the cylindrical geometry prevents a complete scale collapse as was observed in slab geometry in [2].

Conclusions In this paper we have shown that by considering an equilibrium that consists of piecewise uniform generalized vorticities we can obtain an analytical expression for the dispersion relation for linear perturbations.

Furthermore, this approach allows us to apply the powerful contour dynamics methods to study collisionless magnetic reconnection. The results show how analytically determined (in) stability of a cylindrical tearing mode is confirmed by numerical calculation.

Acknowledgments This work, supported by the European Communities under the contract of Association between EURATOM/FOM, was carried out within the framework of the European Fusion Programme with financial support from NWO. The views and opinions expressed herein do not necessarily reflect those of the European Commission.

References.

[1] M. Ottaviani and F. Porcelli, Phys. Rev. Lett. **71**, 3802 (1993).
[2] H.J. de Blank and G. Valori, Plasma Phys. Control. Fusion **45**, A309 (2003).
[3] H.J. de Blank, Phys. Plasmas **8**, 3927 (2001).
[4] P.W.C. Vosbeek and R.M.M. Mattheij, J. Comput. Phys. **133**, 222 (1997).
[5] J.H. Mentink, J. Bergmans, L.P.J.Kamp and T.J. Schep, Phys. Plasmas **12**, 052311 (2005).
[6] T.J. Schep, F. Pegoraro and B.N. Kuvshinov, Phys. Plasmas **1**, nr 9 (1994)
[7] J. Bergmans and T.J. Schep, Phys. Rev. Lett. **87**, nr 19 (2001)